

# The contribution of China's Grain to Green Program to carbon sequestration

Dan Liu · Yang Chen · Wenwen Cai ·  
Wenjie Dong · Jingfeng Xiao · Jiquan Chen ·  
Haicheng Zhang · Jiangzhou Xia · Wenping Yuan

Received: 29 December 2013 / Accepted: 4 August 2014 / Published online: 20 August 2014  
© Springer Science+Business Media Dordrecht 2014

**Abstract** Forests play an important role in regulating atmospheric carbon dioxide concentration and mitigating the greenhouse effect. The Grain to Green Program (GGP) is one of the largest ecological programs in China, and it aims at converting croplands on steep slopes to forests. However, the magnitude and distribution of carbon sequestration induced by GGP remain unknown. In this study, we estimated the changes in carbon fluxes and stocks caused by forests converted from croplands under the GGP using a process-based ecosystem model (i.e., IBIS). Our results showed that the converted areas from croplands

to forests under the GGP program could sequester 110.45 Tg C by 2020, and 524.36 Tg C by the end of this century. The sequestration capacity showed substantial spatial variations with large sequestration in southern China. The economic benefits of carbon sequestration from the GGP were also estimated according to the current carbon price. The estimated economic benefits ranged from \$8.84 to \$44.20 billion from 2000 through 2100, which may exceed the current total investment (\$38.99 billion) on the program. As the GGP program continues and forests grow, the impact of this program will be even larger in the future, making a more considerable contribution to China's carbon sink over the upcoming decades.

D. Liu · Y. Chen · W. Cai · W. Dong ·  
H. Zhang · J. Xia · W. Yuan (✉)  
State Key Laboratory of Earth Surface Processes and  
Resource Ecology, Beijing Normal University,  
Beijing 100875, China  
e-mail: wenpingyuancn@yahoo.com

J. Xiao  
Earth Systems Research Center, Institute for the Study of  
Earth, Oceans, and Space, University of New Hampshire,  
Durham, NH 03824, USA

J. Xiao · J. Chen  
International Center for Ecology, Meteorology, and  
Environment, School of Applied Meteorology, Nanjing  
University of Information Science and Technology,  
Nanjing 210044, Jiangsu, China

J. Chen  
Centre for Global Change & Earth Observations,  
Department of Geography, Michigan State University,  
East Lansing, MI 48823, USA

**Keywords** Grain to Green Program · Integrated  
biosphere simulator · Carbon sequestration ·  
Modeling · Carbon sink

## Introduction

The atmospheric carbon dioxide (CO<sub>2</sub>) concentration has been increasing rapidly since the industrial revolution, particularly during the last three to four decades (Canadell et al. 2007). Among the current policies for carbon (C) mitigation, forest policies can make a significant contribution to a low-cost global mitigation portfolio (Nabuurs et al. 2007). Afforestation and reforestation are major strategies to mitigate C emissions through forest management practices

(Canadell and Raupach 2008). For example, the temperate forests contributed 27 and 34 % to the global C sinks during the 1990s and 2000s respectively (Pan et al. 2011), and the primary reasons for the increased C sinks are the substantial increases in forest area due to afforestation and reforestation and the subsequent increase in vegetation biomass (Birdsey et al. 2006).

The Chinese government implemented several large-scale forestation programs since the 1970s. The Six Key Forestry Programs (e.g., Three Norths Shelter Forest System Project, the Natural Forest Conservation Program and Grain to Green Program) are unprecedented in China's ecological and environmental history in terms of geographic extent, government budget and social mobilization (Dai 2010). These programs have led to a substantial increase in forest area (State Forestry Administration of China (SFA) 2012). According to FAO (2012), there was a net reduction of 13 million hectares (ha) in global forest area between 2000 and 2010, while Asia was the only region with net gains, primarily due to the extensive reforestation and afforestation in China.

The Grain to Green Program (GGP) in China was launched in 1999 to advocates three types of land conversions: croplands to forests, croplands to grasslands, and barren lands to forests on steep slopes by providing farmers food and cash subsidies. This project has been implemented in more than 2,000 counties of 25 provinces (Liu et al. 2008). Large-scale afforestation can result in extensive new forests and hence enhance the carbon sequestration capacity (Niu and Duiker 2006). To date, several studies have assessed the C sequestration of the GGP. Chen et al. (2009) estimated the C sequestration potential in Yunnan province and reported an increase of 12.47 Tg C in the GGP-stands by the year of 2010. Feng et al. (2013) showed that the GGP program sequestered a total of 96.2 Tg C for the period 2000–2008 on the Loess Plateau. Despite these findings, to our knowledge, no study has explicitly assessed the nationwide C sequestration potential of the GGP at decadal to century scales by considering the effects of climate.

In this study, we used the integrated biosphere simulator (IBIS) to assess the magnitude and distribution of the C sequestration resulting from the GGP program. The specific objectives of this study are to: (1) investigate how C fluxes and stocks change under the

GGP initiative; (2) estimate the magnitude of current C sequestration resulting from the GGP; and (3) project the potential C sequestration of the GGP for the future.

## Methods and data

### IBIS model

Process-based ecosystem modeling is a preferred approach to quantify C sequestration of land-use changes over large areas. A process-based model typically has detailed representation of ecosystem processes that ensure its ability to capture and predict the C dynamics caused by land-use changes such as afforestation and forest managements (Pilli et al. 2013). In this study, we used IBIS (Foley et al. 1996; Kucharik et al. 2000; Yuan et al. 2010) to assess the magnitude and distribution of the C sequestration resulting from the GGP. IBIS is a dynamic vegetation model designed to integrate a variety of terrestrial ecosystem phenomena within a single, physically consistent model. It is capable of simulating canopy physiology (canopy photosynthesis and conductance), phenology (budburst and senescence), vegetation dynamics (allocation, turnover, and competition between plant types), and terrestrial C balance (net primary production (NPP), tissue turnover, soil C and organic matter decomposition) (Foley et al. 1996). Driven by daily climatic variables (e.g., temperature, precipitation, cloud fraction and relative humidity), soil texture, and vegetation type, IBIS first interpolates the input climate data to hourly time step using a weather generator, and performs a coupled simulation of the surface water, energy, and carbon fluxes on hourly time step. The model then integrates hourly fluxes over the year to estimate the annual water and carbon balance, and use the annual carbon balance to predict changes in the leaf area index (LAI) and biomass for each vegetation type.

In IBIS, the photosynthesis process is expressed by the Farquhar equations (Farquhar et al. 1980). The photosynthesis rate is calculated at an hourly time step and then integrated to daily and annual time steps:

$$GPP = \int A_g dt \quad (1)$$

where  $A_g$  is the photosynthesis rate ( $\text{mol CO}_2 \text{ m}^{-2} \text{ s}^{-1}$ ) and  $t$  represents time step.

The NPP is calculated as

$$NPP = (1 - \eta) \int (A_g - R_{leaf} - R_{stem} - R_{root}) dt \quad (2)$$

where  $\eta$  (0.33) is the fraction of C lost in the construction of net plant material because of growth respiration (Amthor 1984).  $R_{leaf}$ ,  $R_{stem}$ , and  $R_{root}$  are the respiration rate of leaf, stem and root, respectively.

IBIS uses three C pools to describe biomass: leaves, transport tissues (i.e., predominantly stems), and fine roots. Changes in the biomass pool  $c_i$  are described as:

$$\frac{\partial C_i}{\partial t} = \alpha_i NPP - \frac{C_i}{\tau_i} \quad (3)$$

where  $\alpha_i$  represents the fraction of annual NPP allocated to each biomass compartment and  $\tau_i$  describes the residence time of C in the biomass compartment.

The decomposition of soil organic matter is simulated at a daily time step. The base decay rates of litter, root, and soil C and microbial biomass turnover are modified by soil temperature and soil moisture. C added to the soil through the decomposition process is not partitioned with respect to soil layers (e.g., decomposition of fine root biomass is not kept track of for each individual soil layer); instead, the total amount of decomposed C is aggregated for the total soil profile (Kucharik et al. 2000).

The IBIS does not explicitly simulate the C cycle of crop ecosystems. In this study, we simulated the croplands as grasslands. In order to simulate the GGP process, in which croplands were abandoned and trees were planted, we made the following modifications:

- (1) In the year of executing GGP, we changed the plant functional type (PFT) from cropland to forest, and set the aboveground biomass (leaf biomass and wood biomass) to zero (i.e., removal of the aboveground crops). The belowground biomass of crops was transferred to litter pool.
- (2) The initial biomass of leaf, root and wood of the new planted trees were calculated using the allometric equations of Blujdea et al. (2012). The initial diameter at breast height (DBH) was set as 3 cm. The leaf area index (LAI) was initialized depending on its relationship with leaf biomass:

$$LAI = C_{leaf} \times SLA \quad (4)$$

where  $C_{leaf}$  is the C in leaf biomass, and  $SLA$  is specific leaf area ( $m^2 g^{-1} C$ ).

Two simulations were performed in this study: the Control simulation and the GGP simulation. In both simulations, IBIS was first spin-up for 400 years to achieve the soil C balance by using the climate data from 1960 to 2013. The identified GGP pixels were simulated as croplands in the Control simulation all through the period (400 years for spin-up, and 1960–2100 for simulation). In the GGP simulation, the GGP pixels were simulated as croplands before the year that the GGP was launched and as forests thereafter.

## Data

We used the gridded daily meteorological dataset (temperature, precipitation, cloud fraction and relative humidity) provided by Yuan et al. (2014b). This dataset was based on the meteorological observations from 735 stations from National Climate Center of China Meteorological Administration and were interpolated to a gridded climate dataset with a spatial resolution of  $10 \times 10$  km using the thin plate smoothing splines (Yuan et al. 2014a). The data from stations generally have gaps in time series (i.e., not all stations have record for a specific day), but the fraction of gap-stations was usually small. Thus, during the interpolation, at least 600 meteorological sites have records for the specific day and these sites were used to generate interpolated meteorological dataset. In this study, we used the gridded data for the period 1960–2013 to drive IBIS model. In order to examine the effects of future climate change, meteorological outputs from the Community Climate System Model (CCSM4) at the Representative Concentration Pathways 4.5 (RCP4.5) (Gent et al. 2011) were used. The outputs of CCSM4 are under the standard of Coupled Model Intercomparison Project phase-5 (CMIP5), and the spatial resolution is  $0.94^\circ$  latitude  $\times$   $1.25^\circ$  longitude. To provide soil information for model simulation, the soil texture (e.g., sand and clay content) and soil C content data with spatial resolution of  $0.0083^\circ$  latitude  $\times$   $0.0083^\circ$  longitude were obtained from Shang-Guan et al. (2012, 2013).

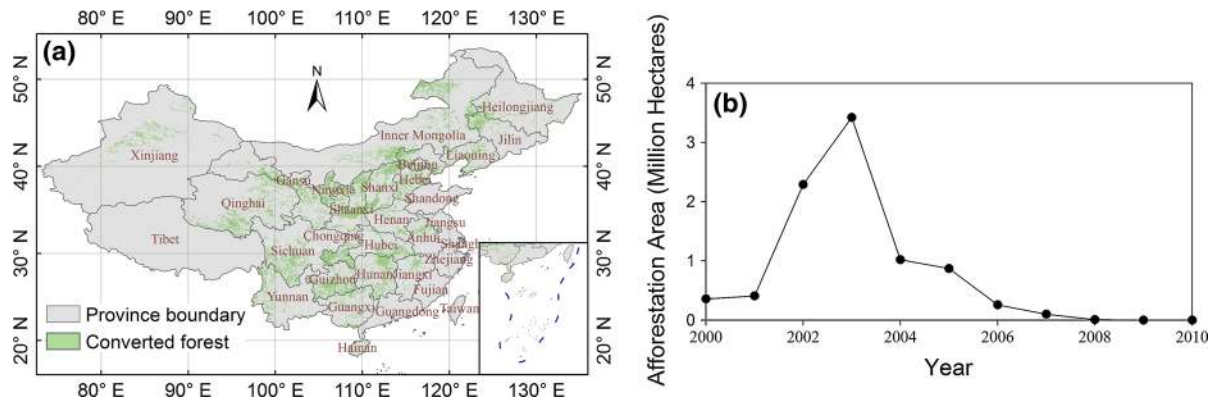


**Fig. 1** The locations of forests converted from croplands under the Grain to Green Program (GGP) (a) and annual area of forests converted from croplands (b). The locations of the GGP were derived from MODIS NDVI products during 2000–2010 at

250-m resolution (Yuan et al. 2014b). The afforestation areas from 2000 to 2010 were obtained from State Forestry Administration of China

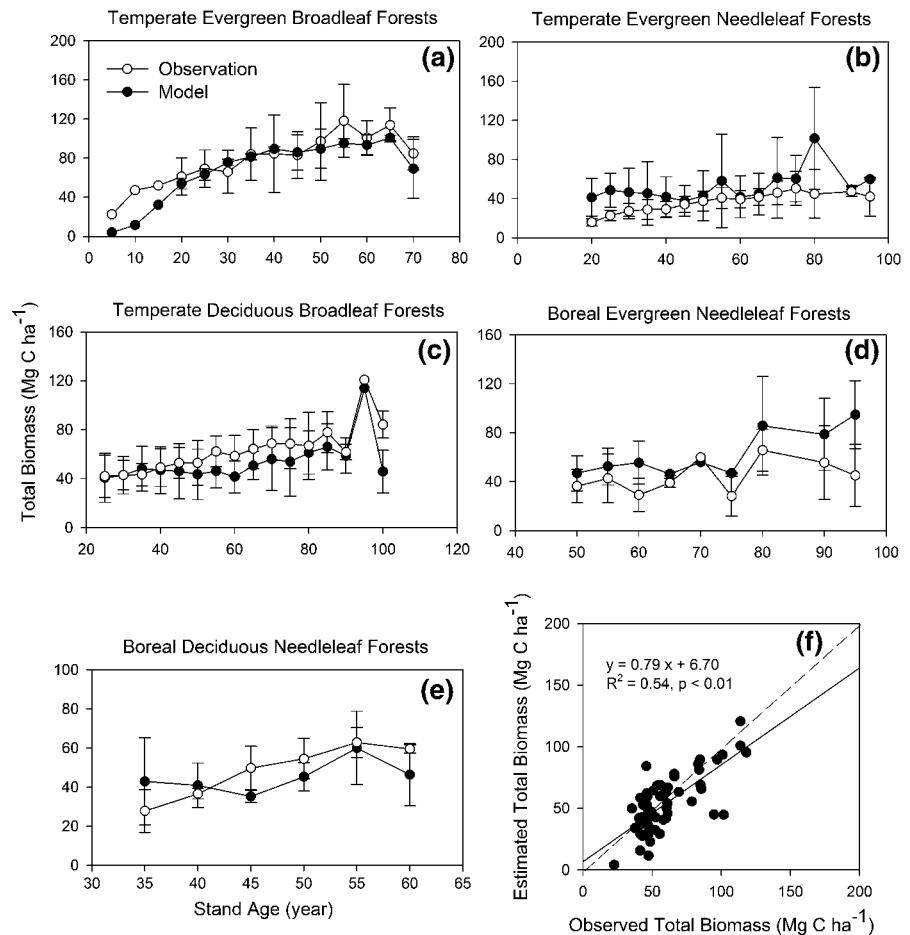
Plant functional types (PFTs) were used in this study to determine the vegetation type of the new planted trees. We combined the Moderate Resolution Imaging Spectroradiometer (MODIS) land cover product (MOD11) with the Köppen-Geiger climate classification scheme to derive a PFT distribution map over China. We assume that the locally dominant tree species would be planted when croplands were converted to forests as these species are likely more adaptable to the local climate. For each GGP pixel, we searched within the 20 km range centered at the pixel for the most frequent PFT, and set it as the PFT of the established forest.

The location-specific data of the GGP was obtained from Yuan et al. (2014b), which characterized the locations of forests converted from cropland under the GGP program from 2000 to 2010 using the Normalized Difference Vegetation Index (NDVI) data derived from MODIS (Fig. 1). The results were validated using the province-level statistics data on the annual afforestation area of GGP project from National Bureau of Statistics of China (<http://www.stats.gov.cn>). These locations only refer to forests converted from croplands, and forests converted from barren lands or grasslands converted from croplands are not included in this study. The GGP maps were at the spatial resolution of  $250 \times 250$  m. As limited by the computational ability, we downgraded the spatial resolution of the GGP maps to  $5 \times 5$  km. For the downgraded GGP map, each  $5 \times 5$  km pixel containing one or more

$250 \times 250$  m pixels was identified as a GGP pixel, and the fraction of the GGP area in each pixel was recorded for calculating the total magnitude of C fluxes and storage at the regional scale. Only the GGP pixels were included for the simulations in this study. In order to drive model at a consistent spatial resolution, all the driving data were resampled to a spatial resolution of  $5 \times 5$  km using the nearest neighbor method.

A biomass dataset derived from the Chinese Ecosystem Research Network including 834 forest plots was used to validate the IBIS predictions (Luo 1996). This dataset covers the forests with stand age ranging from 3 to 98 years and five major forest types, including temperate evergreen broadleaf forests, temperate evergreen needleleaf forests, temperate deciduous broadleaf forests, boreal evergreen needleleaf forests, and boreal deciduous needleleaf forests. It is a valuable validation dataset for evaluating the model's capability to simulate forest growth which is the most important process for determining C cycle under the GGP. We examined the performance of IBIS at all 834 sites. We spin-up the model for 400 years and then conducted transient simulations starting from the year of disturbance (i.e., abandonment of croplands and plantation of trees). We used the Climate Research Unit (CRU) climate dataset from 1901 through 2009 (CRU TS3.10, Harris et al. 2013) to drive IBIS at those 834 sites, and 1901 climate data was used for the years before 1901.

**Fig. 2** The variations of the simulated and observed total biomass with stand age for five forest types (a–e) and the comparison between simulations and observations (f). The data were grouped with 5 years stand-age intervals and the *error bar* shows the standard deviation within the stand-age groups



## Results

### Model validation

We grouped the 834 plot data with 5 years stand-age intervals to illustrate the performance of IBIS for simulating the tree growth after afforestation or disturbance. The simulated biomass over the various stand ages agreed well with the inventory data (Fig. 2). IBIS successfully captured the increasing pattern of biomass with stand age for almost all vegetation types. For example, for temperate deciduous broadleaf forests, the observed biomass increased from 40.0 Mg C ha<sup>-1</sup> at the young stands to 120.0 Mg C ha<sup>-1</sup> at the stand of 95 year old, and the simulated biomass matched the observations well (Fig. 2c). The model showed similar ability for simulating biomass for all forest types, performing slightly better at young stands.

### Impacts of the GGP on C fluxes

The GGP significantly changed ecosystem C fluxes. The annual NPP decreased dramatically from 24.64 to 12.18 Tg C year<sup>-1</sup> for the first year of the GGP and increased rapidly thereafter. After 2020, the total NPP of the GGP area became stable and varied between 29.22 and 36.81 Tg C year<sup>-1</sup>, which was significantly higher than that of the Control simulation (Fig. 3a). On the contrary, the heterotrophic respiration ( $R_h$ ) showed a strong impulse during the initial years after reforestation, and decreased rapidly in the following 10 years to 18.56 Tg C year<sup>-1</sup> in 2010. After that the  $R_h$  gradually increased until reaching nearly the same magnitude as that of the Control simulation (Fig. 3b). Changes of NPP and  $R_h$  jointly determined the dynamics of net ecosystem production (NEP). A substantial reduction of NEP occurred during the early years after the GGP,

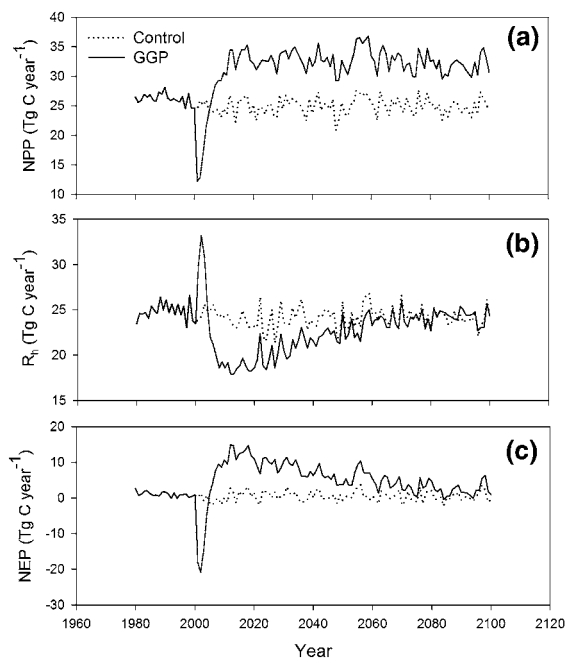


**Fig. 3** Comparison of net primary production (NPP) (a), heterotrophic respiration ( $R_h$ ) (b) and net ecosystem production (NEP) (c) of the Control and GGP simulations over the GGP areas. The *dot* and *solid lines* represent Control and GGP simulations, respectively

and generated a C source of  $18.17 \text{ Tg C year}^{-1}$  in 2001. After 10 years the NEP increased to the maximum of  $14.87 \text{ Tg C year}^{-1}$  in 2012, providing the largest C sink. In the following decades, the C sink gradually weakened and finally reached the carbon neutral stage (Fig. 3c).

The impacts of the GGP on C fluxes showed large spatial variation. Because the annual C fluxes were stable from 2050 to 2100 (Fig. 3), we calculated the differences in fluxes between the Control and the GGP simulations during this period to examine the spatial differences of C fluxes caused by the GGP. Our results showed higher NPP and  $R_h$  for the GGP simulation than for the Control simulation over southern China, especially in Sichuan, Chongqing, Guizhou, Yunnan, and Hunan provinces (Fig. 4a). On the contrary, in northern China, lower NPP and  $R_h$  simulations were found in GGP simulation. Similarly, southern China was found with stronger carbon sink measured by NEP at the GGP simulation compared with the Control simulation, and northern China showed slightly weaker carbon sink (Fig. 4c).

### Impacts of the GGP on C stocks

The GGP program substantially changed both vegetation and soil C pools. The total biomass increased continually since 2,000 and reached  $540.67 \text{ Tg C}$  in 2,100 (Fig. 5a). The soil C declined within the first 20 years and then increased for GGP simulation (Fig. 5b). Over first 20 years, soil C decreased from  $423.03$  to  $367.78 \text{ Tg C}$ . With forest growth, soil C began to increase slowly and reached  $444.33 \text{ Tg C}$  in 2100. Spatially, higher biomass mainly occurred in southern China, especially in Sichuan, Chongqing, and Guizhou province (Fig. 6a). Larger increase of soil C was mainly found in southern China, especially in Guizhou, Chongqing, Hunan and Hubei provinces, and soil C decreased mainly in northern China, especially in Gansu, Shaanxi, Shanxi and Jilin province (Fig. 6b).

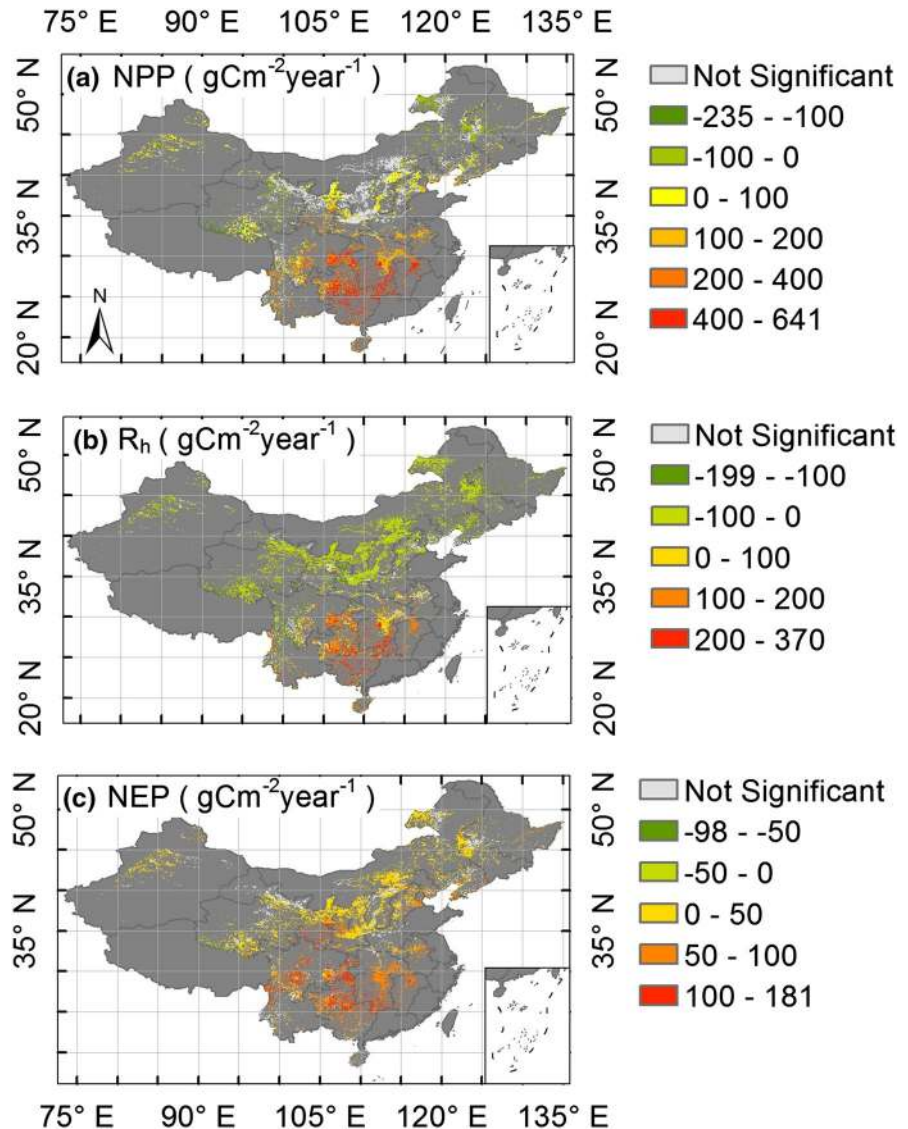
### Carbon sequestration capacity and rate

We calculated the cumulated NEP since 1999 to quantify the magnitude of ecosystem C sequestration resulting from the GGP. We found that the ecosystems did not sequester C during the first decade due to the C loss from the soil C pool, but switched to a net C sink thereafter (Fig. 7). The GGP project could result in a total net C uptake of  $110.46 \text{ Tg C}$  in the first 20 years, and  $524.36 \text{ Tg C}$  by the end of this century, 97.30 % of which was stored in the vegetation C pool (Fig. 7).

At the province level, the top five provinces for C sequestration capacity were Sichuan, Shaanxi, Chongqing, Inner Mongolia and Guizhou (Table 1). The highest rates of annual sequestration occurred in the five southern provinces: Jiangxi, Chongqing, Guangxi, Guizhou and Hainan. All the provinces with lower sequestration rates than the national average rate lie in the northern China. Despite the relatively low rate of sequestration on a per unit area basis, Shaanxi and Inner Mongolia had high total C sequestration capacity because of the extensive area of afforestation from GGP.

The soil C sequestration of most provinces for the first 20 years was negative, indicating that GGP activities had caused soil C loss for the first two decades (Table 2). The largest loss occurred in Inner Mongolia, Shaanxi, Hebei, Sichuan and Shanxi provinces, due to large afforestation area rather than high rate of C loss. After 50 years, several provinces in

**Fig. 4** Spatial distribution of the differences in net primary production (NPP) (a), heterotrophic respiration ( $R_h$ ) (b) and net ecosystem production (NEP) (c) between the GGP and Control simulations from 2050 to 2100



southern China showed positive soil carbon sequestration; by the end of the century, the largest soil C sequestration occurred in Sichuan, Guizhou, Hunan, Chongqing and Yunnan provinces.

## Discussion

### Impacts of the GGP on carbon fluxes and stocks

The GGP program is one of the largest ecological programs in China, and substantial C sequestration is

expected because of its massive scale and the subsequent increase in forest cover. By the end of 2009, the GGP had converted 8.69 million ha of croplands into forests and afforested 15.10 million ha of barren lands (State Forestry Administration of China 2000–2012). As a result, the forest cover within the GGP region has increased by 2 % during 8 years since the program's inception (Liu et al. 2008). The magnitude and spatial distribution of C sequestration associated with such extensive afforestation is of growing interest. As we estimated in this study, the forests converted from croplands under the GGP could

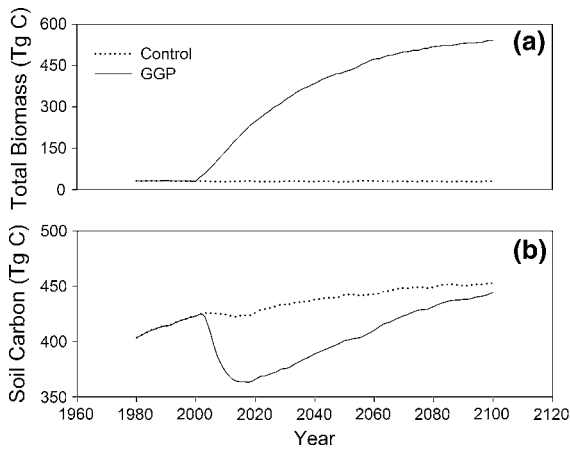


**Fig. 5** Comparison of total biomass (a) and soil carbon (b) of the Control and GGP simulations. The dot and solid lines represent Control and GGP simulations, respectively

sequester 110.46 Tg C in the first two decades and 524.36 Tg C by the end of this century.

Converting croplands to forests could generate rapid C sequestration in biomass. Carbon fixed through photosynthesis is allocated to different tissues of plants (i.e., foliage, fine roots, stems, and grains). In the croplands, irrigation and fertilization prompt C to be allocated in grain which is harvested and consumed and eventually released back into the atmosphere (Génard et al. 2008). While in the forests, C allocated to woody tissues could be stored over time because the woody tissues typically have slow turnover rate (Schulze et al. 2000). In this study, we found that 97.30 % of the absorbed C was stored in biomass (Fig. 7). Several previous studies have been conducted to estimate the contributions from the GGP. Persson

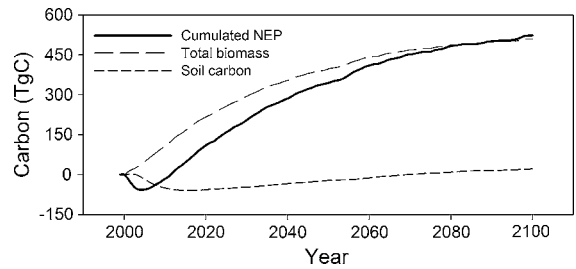


**Fig. 7** Long-term variations of cumulated net ecosystem production (NEP), total biomass and soil carbon

et al. (2013) estimated the C sequestration caused by the GGP from 1999 to 2008 at the national scale based on the forest inventory datasets, which only included the vegetation C sequestration. Our results generally agreed with that of Persson et al. (2013) for 1999–2008 (Fig. 8).

Soil C pool is a major carbon reservoir, and the GGP activities have significantly changed its magnitude. Our simulations showed that soil C decreased for the first two decades after the afforestation and then increased gradually, which was consistent with other studies. Turner and Lambert (2000) analyzed soil organic C in eastern Australia forests and found that net accumulation in the total system did not occur for 10–20 years after plantation establishment. The primary cause of the initial reduction is the low NPP for the young forests and the consequently small amount of litter fall which reduces the C input to the soil. However, this decrease is temporary and in the long-term studies soil C is generally found to accumulate associated with state age (Paul et al. 2002). The estimates from Post and Kwon (2000) showed that soil

**Fig. 6** Spatial distribution of the differences in total biomass (a) and soil carbon (b) between the GGP and Control simulations from 2050 to 2100

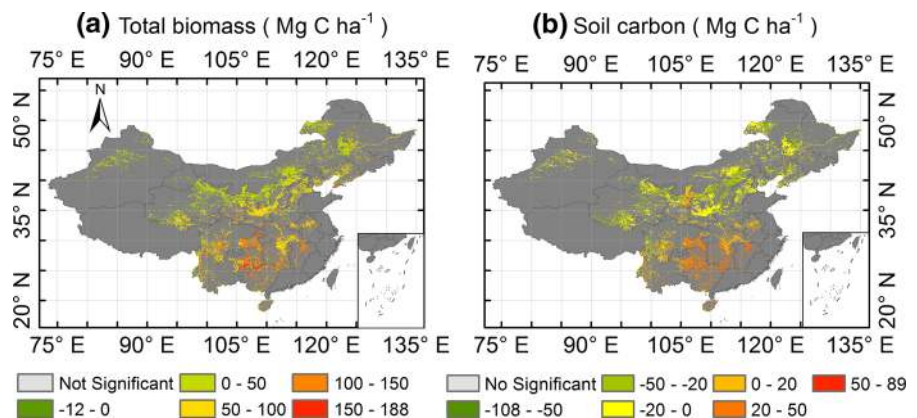




**Table 1** C sequestration capacity and rate by afforestation of cropland within the GGP region over different periods

Province	Area ( $\times 10^4$ ha)	Sequestration capacity (Tg C)			Sequestration rate ( $\text{Mg C ha}^{-1} \text{ year}^{-1}$ )		
		2000–2020	2000–2050	2000–2100	2000–2020	2000–2050	2000–2100
Sichuan	68.75	31.29	60.55	77.48	1.93	1.49	0.96
Shaanxi	77.71	25.36	40.27	52.85	1.52	0.97	0.63
Chongqing	36.16	21.20	39.18	48.27	2.95	2.18	1.34
InnerMongolia	72.04	16.51	29.59	40.76	0.85	0.61	0.42
Guizhou	42.56	15.54	29.29	35.05	2.77	2.09	1.25
Hunan	50.08	13.94	26.09	31.31	2.21	1.66	0.99
Gansu	57.01	9.72	18.06	25.33	0.91	0.68	0.47
Hebei	55.56	8.85	16.87	24.07	1.12	0.86	0.61
Yunnan	33.43	8.82	15.25	17.70	2.08	1.44	0.84
Hubei	32.22	8.55	16.80	20.38	1.69	1.33	0.81
Shanxi	20.00	8.19	14.23	19.42	1.23	0.85	0.58
Guangxi	22.40	7.59	13.64	16.00	2.91	2.09	1.23
Jiangxi	20.00	5.83	11.11	13.62	3.05	2.33	1.43
Qinghai	14.33	5.52	10.31	14.61	0.75	0.56	0.39
Anhui	22.70	5.21	10.40	12.68	1.63	1.30	0.79
Liaoning	19.92	4.87	9.75	12.76	1.52	1.21	0.79
Heilongjiang	24.06	4.83	9.11	11.72	1.49	1.12	0.72
Ningxia	29.56	4.03	7.13	10.15	0.80	0.56	0.40
Henan	23.78	3.87	6.78	8.50	1.60	1.12	0.70
Jilin	22.40	3.67	6.56	8.67	1.08	0.78	0.51
Xinjiang	32.58	1.29	2.28	3.26	0.50	0.35	0.25
Hainan	4.07	0.86	1.31	1.35	2.43	1.47	0.76
Tibet	0.55	0.86	1.67	2.24	1.70	1.33	0.89
Beijing	2.49	0.64	1.23	1.81	1.32	1.02	0.75
Tianjin	10.19	0.22	0.48	0.68	1.25	1.09	0.77
Total	869.24	217.25	397.95	510.67	1.53	1.12	0.72

C could increase by  $0.6\text{--}0.7 \text{ Mg ha}^{-1} \text{ year}^{-1}$  for 50–100 years following afforestation of agricultural land.

Forests sequester  $\text{CO}_2$  from the atmosphere thus afforestation can potentially increase C sink (Nilsson and Schopfhauser 1995). However, during the early years after cropland-to-forest conversion, the ecosystems were found to be strong C sources (Fig. 3). The observations from the disturbed forests (e.g., clear cut or fire disturbance) provide evidence of the disturbance influence on carbon budget changes (Chen et al. 2004). Law et al. (2001) estimated the fluxes of two ponderosa pine forests and found that the young forest was a source of  $\text{CO}_2$  to the atmosphere while the old forest was a C sink. Forest NPP varies predictably with

stand age, and generally shows a rapidly increasing pattern in the young ages, peak growth in the middle ages and slow decline in the mature ages (Pregitzer and Euskirchen 2004). Thus the plantations are expected to have low NPP for the early years. Meanwhile, the soil respiration will increase initially due to the decomposition of C from residues of the preceding agricultural phase (Paul et al. 2002). Therefore in the early years after afforestation, the ecosystem is a C source rather than a sink. This C source, however, will switch to a C sink as the trees grow and forests mature (Chen et al. 2004).

The impacts of the GGP on C budgets showed significant spatial variability across China's landscapes. We found major C sequestration in the warm

**Table 2** Soil C sequestration capacity and rate by afforestation of cropland within the GGP region over different periods

Province	Sequestration capacity (Tg C)			Sequestration rate (Mg C ha <sup>-1</sup> year <sup>-1</sup> )		
	2000–2020	2000–2050	2000–2100	2000–2020	2000–2050	2000–2100
Sichuan	-5.25	6.10	19.81	-0.32	0.15	0.24
Guizhou	-2.13	2.52	6.02	-0.38	0.18	0.21
Hunan	-2.72	1.22	4.87	-0.43	0.08	0.15
Chongqing	-2.27	1.54	4.73	-0.32	0.09	0.13
Yunnan	-2.03	1.08	4.21	-0.48	0.10	0.20
Ningxia	0.35	1.32	2.89	0.07	0.10	0.11
Guangxi	-0.85	0.79	2.29	-0.33	0.12	0.18
Anhui	-1.29	1.13	2.15	-0.40	0.14	0.13
Jiangxi	-0.68	0.36	1.63	-0.36	0.08	0.17
Hubei	-2.78	-0.19	1.61	-0.55	-0.02	0.06
Tibet	0.09	0.63	1.30	0.17	0.50	0.52
Hainan	-0.05	0.08	0.22	-0.15	0.09	0.12
Xinjiang	-0.48	-0.43	0.09	-0.19	-0.07	0.01
Tianjin	-0.12	-0.10	-0.04	-0.69	-0.23	-0.04
Beijing	-0.39	-0.35	-0.25	-0.80	-0.29	-0.10
Henan	-1.34	-0.55	-0.36	-0.55	-0.09	-0.03
Qinghai	-2.12	-1.87	-0.44	-0.29	-0.10	-0.01
Gansu	-4.03	-3.52	-1.27	-0.38	-0.13	-0.02
Liaoning	-1.91	-1.66	-1.40	-0.60	-0.21	-0.09
Jinlin	-1.48	-1.83	-1.76	-0.44	-0.22	-0.10
Heilongjiang	-1.72	-2.44	-2.76	-0.53	-0.30	-0.17
Shanxi	-5.89	-5.39	-3.56	-0.35	-0.13	-0.04
Hebei	-5.67	-6.05	-5.11	-0.72	-0.31	-0.13
Shanxi	-5.05	-6.13	-6.39	-0.76	-0.37	-0.19
InnerMongolia	-7.42	-8.41	-7.17	-0.38	-0.17	-0.07
Total	-57.26	-22.17	21.30	-0.40	-0.06	0.03

and wet southern China. A recent synthesis study showed that the carbon fluxes of China's terrestrial ecosystems were regulated by temperature, precipitation, and growing season length (Xiao et al. 2013), and annual GPP generally declined with increasing latitude (Cai et al. 2014; Li et al. 2013). Feng et al. (2013) demonstrated that climate has significant impact on C sequestration, and they found the vegetation restoration on the Loess Plateau is especially limited by the availability of water. Valentini et al. (2000) analyzed the net ecosystem C exchange in 15 European forests and demonstrated that the more southern, warmer forests sequester more C than the more northerly, cooler forests. Given the high cost of human interventions in such an extensive program, it is therefore particularly important to take the climate factors into account in the development of the program. Future

afforestation efforts should focus on southern China where heat and water are more favorable for tree growth (Xiao et al. 2013).

Climate also strongly impacts soil C accumulation following afforestation. The results showed that soil C increase in southern China where the climate is warm and wet while decrease in northern China where climate is cool and dry (Yuan et al. 2014c). This is consistent with common observations that soil C accumulation increases with increasing mean annual precipitation (Paul et al. 2002; Cooper 1983; Lugo and Sanchez 1986). In humid regions, the forest can keep fast growth rate which lead to high inputs of organic matter to the forest floor, on the contrary, in the dry climate less litter input result in slow soil C recovery (Brown and Lugo 1990).

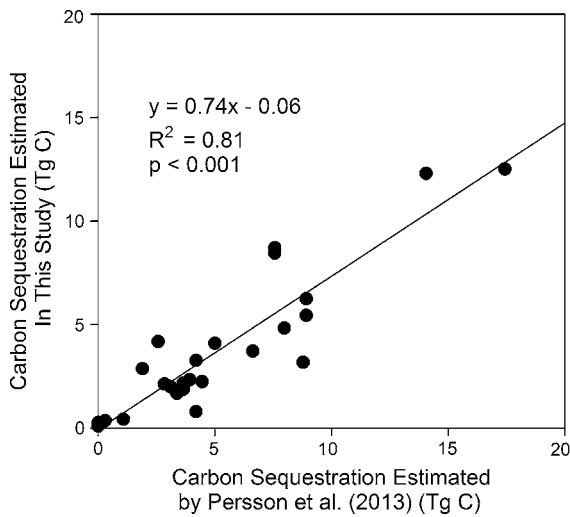


**Fig. 8** Comparison of carbon sequestration by vegetation between Persson et al. (2013) and this study across 25 provinces for the period 2000–2008

After afforestation, a large proportion of the fixed C will be stored in biomass. The C fixed through photosynthesis is allocated to leaves, stems and roots. Stems and coarse roots generally have long turnover time, and a large proportion of the fixed C is stored rapidly in biomass (Schulze et al. 2000). Leaves and branches fall into forest floor as litter (Zhang et al. 2014), which contain large amount of decomposable materials (e.g., celluloses), and are decomposed rapidly. Therefore only a small proportion of C in litter is finally stored in soil. In this study we found that 97.30 % of the fixed C will be stored in biomass, while only 2.70 % C will be accumulated in soil on the national scale. From a four-decade-long field study, Richter et al. (1999) found the similar result that <1 % of the C was accumulated in mineral soil, 80 % in biomass and 20 % in forest floor. From a chronosequence study, Vesterdal et al. (2007) found that the contribution of soil C accumulation to ecosystem C sequestration varied from 0 to 31 %. This rate varies in different spaces, and our results showed that most soil C accumulation occurred in southern China.

#### Economic benefits of the GGP-induced carbon sequestration

Besides the ecological benefits, the economic benefits of the GGP program are also likely considerable.

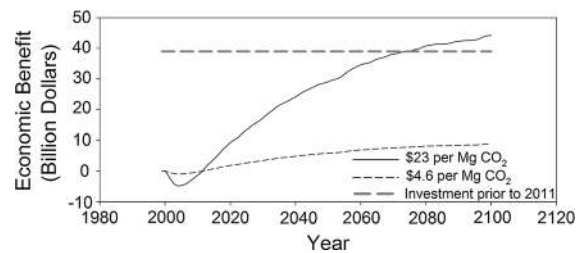


**Fig. 9** The economic benefit of the GGP program at the carbon price of \$23 per Mg CO<sub>2</sub> (solid line) and \$4.6 per Mg CO<sub>2</sub> (short dash line). The coarse long dash line indicates the total investment prior to 2011

China entered the international C market in June, 2013. The C price was initially set to be \$4.6 per Mg CO<sub>2</sub>, and varied roughly in the following 5 months with a peak price of \$23 per Mg CO<sub>2</sub>. Based on this information, the C sequestered through the GGP could generate \$8.84 to \$44.20 billion in 2100 (Fig. 9), which may exceed the current total investment \$38.99 billion (SFA 2012). Moreover, afforestation could lead to substantial economic values of other ecosystem services (e.g., tourism, biodiversity, water and soil conservation, and pollution reduction) (Liu et al. 2008). For example, the total economic value of ecosystem services 4 years after GGP implementation in the 55,300 ha GGP land of Zhangjiajie National Forest Park in Hunan Province was \$70.28 million (Zhuang and Tang 2006). Another case study in Wuqi County of Shaanxi Province found that the economic value from the first 6 years of the GGP was \$0.41 billion (Lai et al. 2006).

#### Uncertainties and limitations

As IBIS does not explicitly simulate the C cycle of crop ecosystems, we estimated croplands as grasslands in the present study, and did not consider the influence from agricultural management. The typical agricultural practices in sloping croplands in China include plowing, fertilization, irrigation, and straw returning, which affect C cycle processes in different ways. Tillage practices generally destroy soil aggregates, and result in the exposure of soil C and rapid decomposition (Balesdent et al. 2000). Fertilization and irrigation are practices that eliminate nutrient and water limits on crop growth and are able to increase vegetation production (Liu et al. 2011). Straw

returning is an effective practice that increases soil C storage (Lu et al. 2008). Ignoring these anthropogenic managements in model simulations may cause some extent of uncertainties, and should be considered in future studies.

In this study, forest disturbances (i.e., harvests, fires and insect breaks) were not integrated into the model simulations. On average, there were only 0.62 % of new planted forests used for timber production and firewood annually (SFA 2000–2012). The ratio of harvested forests to the new planted forests is very low. For the fire disturbances, forest diseases and insect breaks, there are no direct observations on the GGP program. However, according to the China's Forestry Development Reports (SFA 2000–2012), the annual forest area under fire disturbances, diseases and insect breaks was about 3.36 % of the national forest area. Thus we assume that the influence from harvest and disturbance is negligible ( $\sim 4$  %) for the current phase of this program.

The conversion of cropland to forest mainly occurs on the steep slopes where the slopes are  $>25^\circ$ . There are substantial differences in microclimate conditions (temperature, wind speed, precipitation etc.) with the varied topography, which will influence plant growth and soil respiration (Pan et al. 2013). For example, in the Little Laurel Run watershed, trees at the northeast aspect consequently have higher growth rates than those on the southwest slopes because of higher temperature and moisture (Fekedulegn et al. 2003). However, in this national scale study we used the climate driving dataset with  $5 \times 5$  km spatial resolution, and the effects of topography were not explicitly considered into the model simulations. Further studies should be conducted to improve the estimates using higher resolution meteorology dataset.

Another factor that may affect the simulation of vegetation production is the method of calculating LAI. In this study we used the default method in IBIS, which calculates LAI from the leaf biomass and specific leaf area (see method). However, accurate simulation on LAI is a challenge for current models. For example, Anav et al. (2013) examined 18 models participating in the Coupled Model Intercomparison Project phase-5(CMIP5) and found that nearly all models did not capture the spatial and temporal features of LAI and overestimated the global LAI. Therefore, improving the algorithm of LAI in the

future will help to increase the accuracy in simulating vegetation production.

## Conclusions

We assessed the magnitude and distribution of C sequestration resulting from the GGP in China and found that the forests converted from croplands through the GGP could fix 110.45 Tg C by 2020, and 524.36 Tg C by the end of this century, with 97.30 % of which was stored in biomass. The sequestration capacity showed substantial spatial variation with large sequestration in the southern China. The provinces with largest sequestration capacity were Sichuan, Shaanxi, Chongqing, Inner Mongolia and Guizhou. Although in the first two decades after afforestation the ecosystems showed to be C sources, they reversed to C sinks thereafter with the forest regrowth.

The GGP is expected to continue for the coming decades, and this program will likely lead to a larger carbon sink. As the program continues, its impact on carbon sequestration will be greater. The Chinese government has made a future plan for the GGP with a goal of converting 5.33 million ha of croplands and 6.67 million ha of barren land to forests from 2014 to 2020 (State Forestry Administration of China 2013). This additional afforestation is expected to make a larger contribution to the C sink in China for the following decades.

**Acknowledgments** This study was supported by the National Science Foundation for Excellent Young Scholars of China (41322005), National Natural Science Foundation of China (41201078), Program for New Century Excellent Talents in University (NCET-12-0060) and the Fundamental Research Funds for the Central Universities, and the IceMe of NUIST. We thank the anonymous reviewers for their constructive comments on the manuscript.

## References

- Amthor JS (1984) The role of maintenance respiration in plant growth. *Plant Cell Environ* 7(8):561–569
- Anav A, Friedlingstein P, Kidston M, Bopp L, Ciais P, Cox P, Jones C, Jung M, Myneni R, Zhu Z (2013) Evaluating the land and ocean components of the global carbon cycle in the CMIP5 earth system models. *J Clim* 26:6801–6843
- Balesdent J, Chenu C, Balabane M (2000) Relationship of soil organic matter dynamics to physical protection and tillage. *Soil Tillage Res* 53:215–230

- Birdsey R, Pregitzer K, Lucier A (2006) Forest carbon management in the United States: 1600–2100. *J Environ Qual* 35(4):1461–1469
- Blujdea VNB, Pilli R, Dutca I, Ciuvat L, Abrudan IV (2012) Allometric biomass equations for young broadleaved trees in plantations in Romania. *For Ecol Manage* 264:172–184
- Brown S, Lugo AE (1990) Effects of forest clearing and succession on the carbon and nitrogen content of soil in Puerto Rico and US Virgin Islands. *Plant Soil* 124:53–64
- Cai W, Yuan W, Liang S, Zhang X, Dong W, Xia J, Fu Y, Chen Y, Liu D, Zhang Q (2014) Improved estimations of gross primary production using satellite-derived photosynthetically active radiation. *J Geophys Res* 119(1):110–123
- Canadell JG, Raupach MR (2008) Managing Forests for Climate Change Mitigation. *Science* 320(5882):1456–1457
- Canadell JG, Le Quéré C, Raupach MR, Field CB, Buitenhuis ET, Ciais P, Conway TJ, Gillett NP, Houghton RA, Marland G (2007) Contributions to accelerating atmospheric CO<sub>2</sub> growth from economic activity, carbon intensity, and efficiency of natural sinks. *Proc Natl Acad Sci* 104(47):18866–18870
- Chen JQ, Brososke KD, Noormets A, Crow TR, Bresee MK, Le Moine JM, Euskirchen ES, Mather SV, Zheng D (2004) A working framework for quantifying carbon sequestration in disturbed land mosaics. *Environ Manage* 34(3):S210–S221
- Chen XG, Zhang XQ, Zhang YP, Wan CB (2009) Carbon sequestration potential of the stands under the Grain for Green Program in Yunnan Province, China. *For Ecol Manag* 258(3):199–206
- Cooper CF (1983) Carbon storage in managed forests. *Can J For Res* 13(1):155–166
- Dai ZG (2010) Intensive agropastoralism: dryland degradation, the Grain-to-Green Program and islands of sustainability in the Mu Us Sandy Land of China. *Agric Ecosyst Environ* 138(3–4):249–256
- FAO (2012) Global forest land-use change 1990–2005. In: Lindquist EJ, D'Annunzio R, Gerrand A, MacDicken K, Achard F, Beuchle R, Brink A, Eva HD, Mayaux P, San-Miguel-Ayanz J, Stibig H-J (Eds) FAO forestry paper No. 169. Food and agriculture organization of the United Nations and European Commission Joint Research Centre. Rome, FAO
- Farquhar GD, Caemmerer S, Berry JA (1980) A biochemical model of photosynthetic CO<sub>2</sub> assimilation in leaves of C<sub>3</sub> species. *Planta* 149(1):78–90
- Fekedulegn D, Hicks RR, Colbert JJ (2003) Influence of topographic aspect, precipitation and drought on radial growth of four major tree species in an Appalachian watershed. *For Ecol Manage* 177(1–3):409–425
- Feng S, Hu Q, Qian W (2004) Quality control of daily meteorological data in China, 1951–2000: a new dataset. *Int J Climatol* 24:853–870
- Feng XM, Fu BJ, Lu N, Zeng Y, Wu BF (2013) How ecological restoration alters ecosystem services: an analysis of carbon sequestration in China's Loess Plateau. *Scientific Reports* 3
- Foley JA, Prentice IC, Ramankutty N, Levis S, Pollard D, Sitch S, Haxeltine A (1996) An integrated biosphere model of land surface processes, terrestrial carbon balance, and vegetation dynamics. *Global Biogeochem Cycles* 10(4):603–628
- Génard M, Dauzat J, Franck N, Lescourret F, Moitrier N, Vaast P, Vercambre G (2008) Carbon allocation in fruit trees: from theory to modelling. *Trees* 22:269–282
- Gent PR, Danabasoglu G, Donner LJ, Holland MM, Hunke EC, Jayne SR, Lawrence DM, Neale RB, Rasch PJ, Vertenstein M, Worley PH, Yang ZL, Zhang MH (2011) The community climate system model version 4. *J Clim* 24(19):4973–4991
- Harris I, Jones PD, Osborn TJ, Lister DH (2013) Updated high-resolution grids of monthly climatic observations—the CRU TS3.10 dataset. *Int J Climatol* 34(3):623–642
- Kucharik CJ, Foley JA, Delire C, Fisher VA, Coe MT, Lenters JD, Young-Molling C, Ramankutty N, Norman JM, Gower ST (2000) Testing the performance of a dynamic global ecosystem model: water balance, carbon balance, and vegetation structure. *Global Biogeochem Cycles* 14(3):795–825
- Lai Y, Zhu Q, Zhang Y, Qin W, Li W (2006) Valuing ecological effects of Grain to Green Program in Wuqi County. *J Soil Water Conserv* 20:83–87 (In Chinese)
- Law BE, Thornton PE, Irvine J, Anthoni PM, Van Tuyl S (2001) Carbon storage and fluxes in ponderosa pine forests at different developmental stages. *Glob Change Biol* 7(7):755–777
- Li X, Liang S, Yu G, Yuan W, Cheng X, Xia J, Zhao T, Feng J, Ma Z, Ma M, Liu S, Chen J, Shao C, Li S, Zhang X, Zhang Z, Chen S, Ohta T, Varlagin A, Miyata A, Takagi K, Saito N, Kato T (2013) Estimation of gross primary production over the terrestrial ecosystems in China. *Ecol Model* 261–262:80–92
- Liu JG, Li SX, Ouyang ZY, Tam C, Chen XD (2008) Ecological and socioeconomic effects of China's policies for ecosystem services. *Proc Natl Acad Sci* 105(28):9477–9482
- Liu C, Wang K, Meng S, Zheng X, Zhou Z, Han S, Chen D, Yang Z (2011) Effects of irrigation, fertilization and crop straw management on nitrous oxide and nitric oxide emissions from a wheat-maize rotation field in northern China. *Agric Ecosyst Environ* 140(1–2):226–233
- Lu F, Wang X, Han B, Ou-Yang Z, Duan X, Zheng H, Miao H (2008) Soil carbon sequestrations by nitrogen fertilizer application, straw return and no-tillage in China's cropland. *Glob Change Biol* 15(2):281–305
- Lugo AE, Sanchez MJ (1986) Land use and organic carbon content of some subtropical soils. *Plant Soil* 96:185–196
- Luo TX (1996) The spatial pattern and mathematical model of productions of China's major forest types. Unpublished doctoral dissertation. Science Academy of China, Beijing, China
- Nabuurs GJ, Masera O, Andrasko K, Benitez-Ponce P, Boer R, Dutschke M, Elsiddig E, Ford-Robertson J, Frumhoff P, Karjalainen T, Krankina O, Kurz WA, Matsumoto M, Oyhantcabal W, Ravindranath NH, Sanz-Sanchez MJ, Zhang X (2007) Forestry. In Metz B, Davidson OR, Bosch PR, Dave R, Meyer LA (Eds) *Climate Change 2007: Mitigation. Contribution of Working Group III to the Fourth Assessment Report of the Intergovernmental Panel on Climate Change*. Cambridge, United Kingdom and New York, NY, USA

- Nilsson S, Schopfhauser W (1995) The carbon-sequestration potential of a global afforestation program. *Clim Chang* 30(3):267–293
- Niu XZ, Duiker SW (2006) Carbon sequestration potential by afforestation of marginal agricultural land in the Mid-western U.S. *For Ecol Manage* 223(1–3):415–427
- Pan YD, Birdsey RA, Fang JY, Houghton R, Kauppi PE, Kurz WA, Phillips OL, Shvidenko A, Lewis SL, Canadell JG, Ciais P, Jackson RB, Pacala SW, McGuire AD, Piao SL, Rautiainen A, Sitch S, Hayes D (2011) A large and persistent carbon sink in the world's forests. *Science* 333(6045):988–993
- Pan YD, Birdsey RA, Phillips OL, Jackson RB (2013) The Structure, Distribution, and Biomass of the World's Forests. *Annu Rev Ecol Evol Syst* 44:593–622
- Paul KI, Polglase PJ, Nyakuengama JG, Khanna PK (2002) Change in soil carbon following afforestation. *For Ecol Manage* 168:241–257
- Persson M, Moberg J, Ostwald M, Xu J (2013) The Chinese Grain for Green Programme: assessing the carbon sequestered via land reform. *J Environ Manage* 126:142–146
- Pilli R, Grassi G, Kurz WA, Smyth CE, Blujdea V (2013) Application of the CBM-CFS3 model to estimate Italy's forest carbon budget, 1995–2020. *Ecol Model* 266:144–171
- Post WM, Kwon KC (2000) Soil carbon sequestration and land-use change: processes and potential. *Glob Chang Biol* 6(3):317–327
- Pregitzer KS, Euskirchen ES (2004) Carbon cycling and storage in world forests: biome patterns related to forest age. *Glob Chang Biol* 10(12):2052–2077
- Richter DD, Markewitz D, Trumbore SE, Wells CG (1999) Rapid accumulation and turnover of soil carbon in a re-establishing forest. *Nature* 400:56–58
- Schulze ED, Wirth C, Heimann M (2000) Managing forest after Kyoto. *Science* 289(5487):2058–2059
- Shang-Guan W, Dai YJ, Liu BY, Ye AZ, Yuan H (2012) A soil particle-size distribution dataset for regional land and climate modelling in China. *Geoderma* 171–172:85–91
- Shang-Guan W, Dai YJ, Liu BY, Zhu AX, Duan QY, Wu LZ, Ji DY, Ye AZ, Yuan H, Zhang Q, Chen DD, Chen M, Chu JT, Dou YJ, Guo JX, Li HQ, Li JJ, Liang L, Liang X, Liu HP, Liu SY, Miao CY, Zhang YZ (2013) A China data set of soil properties for land surface modeling. *J Adv Model Earth Syst* 5(2):212–224
- State Forestry Administration of China (2013) Grain for Green Program: Looking Forward to restart, from <http://tghl.forestry.gov.cn/portal/tghl/s/3815/content-617743.html>
- State Forestry Administration of China (SFA) (2000–2012) China's Forestry Development Report. Chinese Forestry Publishing House, Beijing, China
- Turner J, Lambert M (2000) Change in organic carbon in forest plantation soils in eastern Australia. *For Ecol Manage* 133(3):231–247
- Valentini R, Matteucci G, Dolman AJ, Schulze ED, Rebmann C, Moors EJ, Granier A, Gross P, Jensen NO, Pilegaard K, Lindroth A, Grelle A, Bernhofer C, Grünwald T, Aubinet M, Ceulemans R, Kowalski AS, Vesala T, Rannik U, Berbigier P, Loustau D, Gümundsson J, Thorgeirsson H, Ibrom A, Morgenstern K, Clement R, Moncrieff J, Montagnani L, Minerbi S, Jarvis PG (2000) Respiration as the main determinant of carbon balance in European forests. *Nature* 404(6780):861–865
- Vesterdal L, Rosenqvist L, Van der Salm C, Hansen K, Groenbergh B-J, Johansson M-B (2007) Carbon sequestration in soil and biomass following afforestation: experiences from oak and Norway spruce chronosequences in Denmark, Sweden and the Netherlands. In: Hansen K, Heil GW, Muys B (eds) Environmental effects of afforestation in North-Western Europe pland and vegetation. Springer, Netherlands, pp 19–51
- Xiao JF, Sun G, Chen J, Chen H, Chen S, Dong G, Gao S, Guo H, Guo J, Han S, Kato T, Li Y, Lin G, Lu W, Ma M, McNulty S, Shao C, Wang X, Xie X, Zhang X, Zhang Z, Zhao B, Zhou G, Zhou J (2013) Carbon fluxes, evapotranspiration, and water use efficiency of terrestrial ecosystems in China. *Agric For Meteorol* 182–183:76–90
- Yuan WP, Liu SG, Liu HP, Randerson JT, Yu GR, Tieszen LL (2010) Impacts of precipitation seasonality and ecosystem types on evapotranspiration in the Yukon River Basin, Alaska. *Water Resour Res* 46(2):2010. doi:10.1029/2009WR008119
- Yuan WP, Xu B, Chen ZQ, Xia JZ, Xu WF, Chen Y, Wu XX, Fu Y (2014a) Validation of China-wide interpolated daily climate variables from 1960 to 2011. *Theoret Appl Climatol*. doi:10.1007/s00704-014-1140-0
- Yuan WP, Li XL, Liang SL, Cui XF, Dong WJ, Liu SG, Xia JZ, Chen Y, Liu D, Zhu WQ (2014b) Characterization of locations and extents of afforestation from the Grain for Green Project in China. *Remote Sens Lett* 5(3):221–229
- Yuan W, Liu D, Dong W, Liu S, Zhou G, Yu G, Zhao T, Feng J, Ma Z, Chen J, Chen Y, Chen S, Han S, Huang J, Li L, Liu H, Liu S, Ma M, Wang Y, Xia J, Xu W, Zhang Q, Zhao X, Zhao L (2014c) Multiyear precipitation reduction strongly decreases carbon uptake over northern China. *J Geophys Res* 119(5):881–896
- Zhang H, Yuan W, Dong W, Liu S (2014) Seasonal patterns of litterfall in forest ecosystem worldwide. *Ecol Complex*. doi:10.1016/j.ecocom.2014.01.003
- Zhuang D, Tang X (2006) Ecological-economic effects of Grain to Green Program in Zhangjiajie. *J Mt Sci* 24:373–377